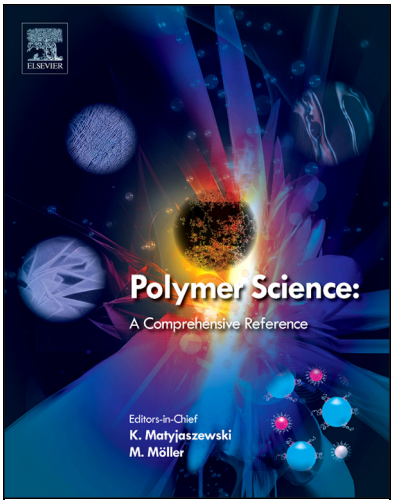

Beaucage G (2012) Combined Small-Angle Scattering for Characterization of Hierarchically Structured Polymer Systems over Nano-to-Micron Meter: Part II Theory. In: Matyjaszewski K and Möller M (eds.) *Polymer Science: A Comprehensive Reference*, Vol 2, pp. 399–409. Amsterdam: Elsevier BV.

2.14 Combined Small-Angle Scattering for Characterization of Hierarchically Structured Polymer Systems over Nano-to-Micron Meter: Part II Theory

G Beaucage, University of Cincinnati, Cincinnati, OH, USA

2.14.1 Introduction

Small-angle scattering from complex structures often involves understanding the relationship between related structural features observed at different size scales. Traditional scattering functions and even traditional approaches are generally not sufficiently flexible to describe complex hierarchical structures. Over the past two decades, an approach has been developed that allows for coupling of simple and general scattering laws to describe hierarchical structures with a great degree of flexibility. This unified function[1,2] results in a generic parameterization of scattering patterns. The function can be linked to structural models in order to limit the fitting parameters and to understand the fitting results. The approach is to apply a general scattering function adaptable to any number of hierarchical levels and to limit the parameters in this function based on the interpretation of structural models in the context of this general scattering function. This approach diverges from the traditional approach in scattering that considers the Fourier transform of a specific structural correlation function based on a model structure or the inverse process involving analysis of an inverse Fourier transform of the scattering measurement. For complex hierarchical systems where a discrete structural model is not available, the unified approach often offers the only reasonable approach to understand small-angle scattering. The unified function offers the opportunity to resolve scattering features obscured by the overlap of structural levels.

2.14.2 Structural Levels

In describing small-angle scattering from hierarchical structures, it is useful to define a base unit of structure as a structural level. A structural level displays a single average and finite structural size defined by a radius of gyration and an associated structural scaling regime that quantifies the statistical structural nature of the level. Many hierarchical structures can be described by a series of structural levels. For example, a polymer gel following the gel tensile-blob (GTB) model[3,4] displays three structural levels, the Kuhn unit, the tensile coil, and the extended structure (Figure 1). On the smallest scale, the Kuhn unit or persistent unit is common to scattering from all polymer systems based on linear chains in dilute solution and reflects local chain rigidity associated with chemical bonds, steric considerations, and other factors that can affect chain stiffness, such as local charge. The Kuhn/persistent unit displays the structural scaling of a rod. That is, from the Kuhn length to the smallest observable sizes in X-ray or neutron scattering, the mass of the Kuhn segment scales with the size of observation to the power 1. In the GTB model, Kuhn units compose local coil structures (Figure 1) governed in size, ξ, by a balance between conformational entropy, enthalpy of interaction between the solvent and the polymer, and the network connectivity. This second structural level displays a scaling regime where mass scales with size of observation by approximately the power 5/3 following good-solvent scaling. In equilibrium-swollen gels, a third structural level is observed that reflects a regime dominated by large-scale stresses on the network associated with swelling. In this regime, swelling forces applied over large distances provide sufficient torque to overcome entropically driven randomization of the structure and a second low-q regime of linear scaling is observed. Figure 2 shows typical scattering from an equilibrium-swollen, end-linked polydimethyl siloxane (PDMS) gel that displays two of the three scaling regimes discussed above. In PDMS, the persistence length, 2.5 Å, is too small to be observed at high q.

The unified approach to the analysis of complex hierarchical structures relies, in the most part, on our ability to quantify the radius of gyration, R_g, and power-law scaling regimes that can be observed in scattering through Guinier's law,

$$I(q) = G \exp\left(\frac{-q^2 R_g^2}{3}\right) \quad [1]$$

and a generalized Porod's law,

$$I(q) = Bq^{-P} \quad [2]$$

Here G reflects the contrast and includes the number concentration of structural units described by R_g, as well as the square of the number of electrons (or another basic unit of scattering)

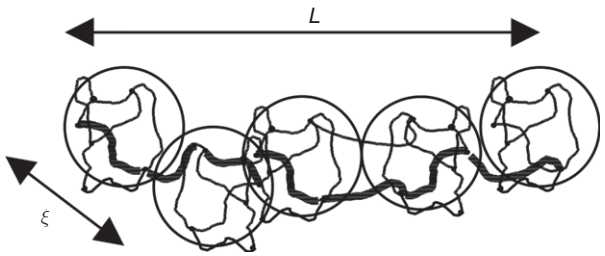

Figure 1 Two structural levels of the gel tensile-blob model. Shown are the tensile coil, ξ, and the extended tensile structure, L. Adapted from Sukumaran, S. K.; Beaucage, G. *Europhys. Lett.* **2002**, *59*, 714–720, Figure 1.[3] Tension on the chain overcomes entropy-driven chain disorder at large scales resulting in a linear structure that is random at scales smaller than the tensile-blob size, ξ.

per structural unit. In eqn [2], B reflects the contrast as well as characteristic sizes specific to the type of structure, while P reflects the nature of the structure and is interpreted differently in two conditions. For P larger than 3, we observe surface scattering with the special case of $P = 4$ for smooth, sharp interfaces (Porod's law), and for P smaller than 3, we observed mass-fractal scaling, which is the general condition for polymers in dilute solution and reflects all three of the structural levels mentioned for a polymer gel.

There are several disadvantages to the direct application of eqns [1] and [2] in the analysis of scattering data from hierarchical systems. For eqn [1], the regime of strict applicability is somewhat narrow and is defined by R_g, so that one needs to guess R_g in order to determine the fitting range and the fitting range affects the resulting R_g. In a hierarchical structure, at low q, the next larger structural level interferes, often to totally obscure the range of applicability, and at higher q, eqn [2] obscures the functionality of eqn [1]. Power-law equations, such as eqn [2], are generally applicable only when one or more decades of power-law scaling can be observed and the limiting values for q are also ill-defined. Then, while eqns [1] and [2] are quite general in theory, in actual use they are limited, and these limitations can lead to errors in quantification of scattering data when they are unreasonably applied, especially in regimes of overlap.

For these reasons, it is desirable to define first a scattering equation that can incorporate eqns [1] and [2] in a nonexclusive manner over a wide range of scattering vector, and second, to describe the combination of scattering functions from local structural levels to describe a hierarchy such as that observed in polymer gels. In the context of this scattering framework, limitations can be placed on the values of G, R_g, B, and P depending on our understanding of structural models. For example, the four fitting parameters for the Kuhn or persistence level of a gel are fully described by a single fitting parameter, the Kuhn length or persistence length,[5,6] if the chemical composition and concentration of the polymer and solvent are known. This size is of importance since it reflects the base, zero conformational entropy unit for thermodynamic and rheological calculations. The Kuhn length can be obtained from first principles using the rotational isomeric states model[7] so that the first structural level could be wholly predetermined.

A number of analytic and empirical functions have been proposed that describe a single structural level, that is, the combination of eqns [1] and [2], for specific structural models. For fractal and polymer systems, the most important of these equations is that of Debye for a Gaussian polymer chain,

$$I(q) = \frac{2G}{q^4 R_g^4}\left(\exp\left(-q^2R_g^2\right) - \left(1 - q^2R_g^2\right)\right) \qquad [3]$$

For this equation, at high q, $B = 2G/R_g^2$ and $P = 2$ for the two-dimensional (2D) random coil. Unfortunately, Debye's approach cannot be generalized in a discrete form to

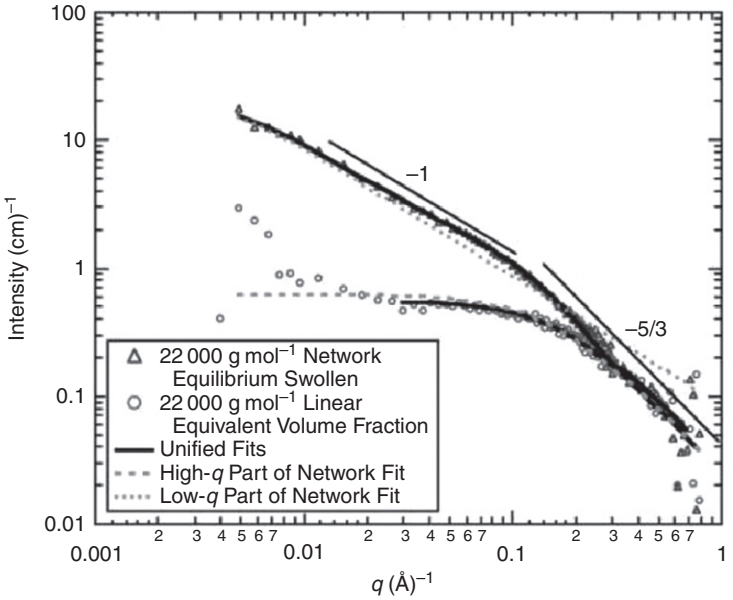

Figure 2 Small-angle neutron scattering from a 22 000 g mole^{-1} end-linked PDMS equilibrium-swollen network in D-benzene and its equivalent PDMS solution. The data are from Argonne National Laboratories, Intense Pulsed Neutron Source, SAND instrument. Fits are to the unified equation using the GTB model. Adapted from Sukumaran, S. K.; Beaucage, G.; Mark, J. E.; Viers, B. *Eur. Phys. J. E* **2005**, *18*, 29–36, Figure 2.[4] At low q (large size scales), an extended linear regime is observed that displays a –1 power-law decay. At smaller size scales (larger q), a self-avoiding walk is observed that displays a –5/3 power-law decay agreeing with the structure shown in **Figure 1**.

dimensions other than two such as in good-solvent scaling, which is the most common condition for polymers in solution. Benoit[8] has extended eqn [3] to account for branched polymers in Gaussian conditions and has presented an integral equation based on eqn [3] that can account for arbitrary mass-fractal dimension.[9] The approach of eqn [3] was also used to describe the scattering from cyclic polymers using an integral equation by Cassasa,[10] though the Cassasa function has recently been brought into question.[11] The empirical Ornstein–Zernike equation is often substituted for eqn [3] since it is of a simpler form, but it displays an incorrect extrapolated value for B at high q. Other empirical functions targeting arbitrary mass-fractal dimensions based on the arbitrary Debye–Bueche 'cut-off function',[12,13]

$$\gamma(r) = \exp\left(\frac{-r}{\xi}\right) \quad [4]$$

have also been proposed.[14–18] The appropriateness of these empirical equations are discussed in a recent article by Rai *et al.*[19]

Single structural levels for three-dimensional (3D) objects have been obtained by direct Fourier transform of calculated correlation functions. The simplest and most widely used of these is the sphere scattering function given by,

$$I(q) = G\left\{\frac{3(\sin qR - qR\cos qR)}{(q^3R^3)}\right\}^2 \quad [5]$$

where $R_g^2 = 3/5R^2$ and R is the radius of the sphere. At high q, this function extrapolates to eqn [2] with $P = 4$ and $B = 9G/R^4 = 25G/R_g^4$.

Debye and Bueche[12] proposed an empirical function to describe scattering from disordered 3D systems that is widely used for particles displaying Porod scaling. The Debye–Bueche empericism (obtained from the *ad hoc* correlation function, eqn [4]) has been generalized to arbitrary surface-fractal dimension,

$$I(q) = G(1 + q^2\xi^2)^{-(6-d_s)/2} \quad [6]$$

where d_s is the surface-fractal dimension and $d_s = 2$ for the Debye–Bueche empericism. Through an extrapolation to low q and comparison with eqn [1], $\xi^2 \cong 2R_g^2/3(6-d_s)$. However, eqn [6] is obtained for $d_s = 2$ from a correlation function with no physical meaning and is further empirically extended for other surface-fractal dimenisons, so the functional form is probably incorrect except in gross features. ξ has no real physical meaning in this equation.[19]

For complex structures such as native-state proteins and other 3D biological structures, the direct Fourier transform of calculated structures is possible and the inverse transform of scattering can be used to obtain a correlation function that can be further analyzed corroborating a molecular model using knowledge from NMR and X-ray diffraction.[20,21] In some cases, it is possible to perform an inverse transform on the scattering data and obtain a correlation function that can be analyzed in terms of gross features. Generally, such an analysis is limited to a single structural level and the connection between features in the measured scattering curve and those in the resulting analysis is lost. Further, data manipulation including extrapolation to high and low q, truncation, and smoothing may introduce artifacts in the results.

2.14.3 Unified Function

A general approach to the description of structural levels in scattering was analytically derived in 1995[1] and is widely used for the analysis of hierarchical systems. The unified function is based directly on eqns [1] and [2],

$$I(q) = G\exp\left(\frac{-q^2R_g^2}{3}\right) + B(q^*)^{-P} \quad [7]$$

where,

$$q^* = \frac{q}{\left\{erf\left(\frac{kqR_g}{\sqrt{6}}\right)\right\}^3} \quad [8]$$

and k has an approximate value of 1.06 for $P = 2$ and 1 for $P > 3$.[22] Figure 3 shows a calculation using eqn [7] for a

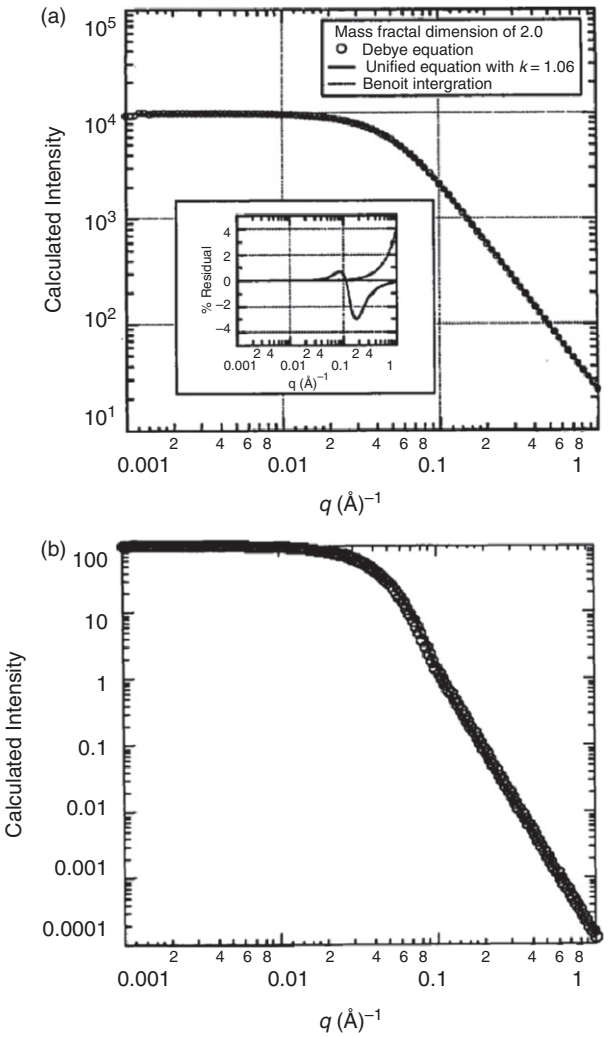

Figure 3 Log–log plots of $I(q)$ vs. q for the unified function for (a) Debye equation for Gaussian polymer coils (eqn [3]) using $B = 2G/R_g^2$. Adapted from Beaucage, G. *J. Appl. Cryst.* **1996**, *29*, 134–146, Figure 1.[22] (b) Polydisperse spheres following eqn [5]. Adapted from Beaucage, G. *J. Appl. Cryst.* **1995**, *28*, 717–728, Figure 11.[1] In both cases, the dark line is the calculated unified function and the points are direct calculations from structural models.

Gaussian, fractal chain (eqn [3]) and for a population of 3D spheres (eqn [5]), demonstrating that the unified function can be applied to both fractal and nonfractal structures representative of two generally exclusive categories of structure in small-angle scattering.

Equation [7] can be extended to describe correlated systems,[2,23]

$$I(q) = \frac{\left(G\exp\left(\frac{-q^2R_g^2}{3}\right) + B(q^*)^{-P}\right)}{1 + p\theta(q)} \quad [9]$$

where,

$$\theta(q) = 3\frac{\sin q\varsigma - q\varsigma\cos q\varsigma}{(q\varsigma)^3} \quad [10]$$

and ζ is the correlation length corresponding to the average distance between spherically correlated particles and p is the packing factor that is 8 times the ratio of the occupied to the available volume. p has a maximum value of 5.92 for closest packed structures. Equation [10] is the amplitude function for spherical scattering, indicating that the domains are loosely arranged in spherical shells. Larger values of the packing factor, p, are possible for nonspherical packing such as for lamellar stacking but an alternative to eqn [10] is needed under these conditions such as integral amplitude functions for lamellar structure. Figure 4 shows a fit to $I(q)$ obtained by small-angle X-ray scattering (SAXS) of correlated silica particles in a polydimethyl siloxane elastomer matrix using eqn [9].

2.14.4 Hierarchy of Structural Levels

For hierarchical systems composed of 'n' structural levels, eqn [7] is extended using the Guinier function as described by Beaucage,[1]

$$I(q) = \sum_{i=1}^{n}\left(G_i\exp\left(\frac{-q^2R_{g,i}^2}{3}\right) + B_i\exp\left(\frac{-q^2R_{g,i+1}^2}{3}\right)q^{*P_i}\right) \quad [11]$$

where,

$$q^* = \frac{q}{\left\{erf\left(\frac{kqR_{g,i}}{\sqrt{6}}\right)\right\}^3} \quad [12]$$

Equation [11] implies that each succeeding structural level (larger in size as the index increases) is composed wholly from the previous, smaller level. For example, a fractal aggregate displays a primary structural level ($i = 1$) composed of particles with a Porod-scaling regime. These primary particles completely compose an aggregate structure that may be randomly branched in a second structural level ($i = 2$). The second structural level would display a fractal-scaling regime. Aggregates often cluster into agglomerates, which display a second Porod or surface-fractal-scaling regime at low q ($i = 3$). Figure 5 shows a schematic of two structural levels, as well as self-similarity in the fractal regime (central sketch).

An equilibrium-swollen polymer gel[3,4] also displays a hierarchical structure generally beginning with the Kuhn segment ($i = 1$), proceeding to the tensile coil ($i = 2$) and the extended structure ($i = 3$) as discussed above. Each succeeding hierarchical level is wholly composed of the previous level. In some cases, a structural level is not part of the hierarchical tree. For example, a polymer gel might contain bubbles that display Porod scaling. Such unrelated structures could be added to eqn [11] if there is no significant correlation between the position of the unrelated structures and that of the hierarchical structure, that is, if the bubbles do not decorate the polymer or otherwise interact with the polymeric structure.

2.14.5 Structural Models and the Unified Function

Equation [11] offers a new method for the analysis of small-angle scattering since application of eqn [11] to complex structural systems does not require calculation of the correlation function. In this way, eqn [11] offers a direct interpretation of scattering data based on our understanding of eqns [1] and [2] in the context of specific structural models. Several examples are discussed below.

The main goal in applying eqn [11] is to couple a structural model with the scattering function so as to reduce the number

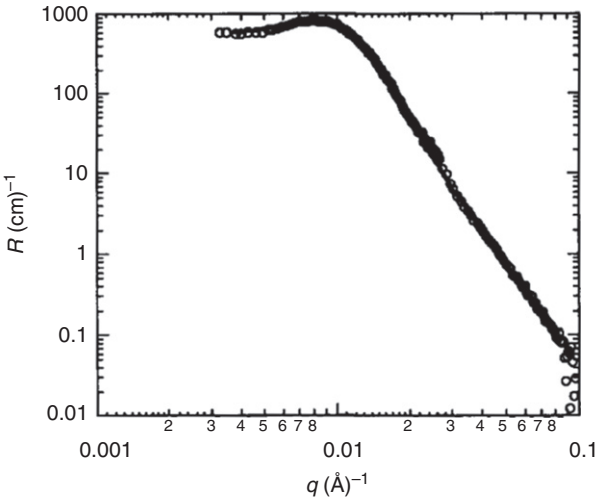

Figure 4 Fit of eqn [9] to SANS data (dark line) from a siloxane rubber filled with silica particles. Adapted from Beaucage, G.; Schaefer, D. W. *J. Non-Cryst. Solids* **1994**, *172–174*, 797–805, Figure 10.[2] The data display a correlation peak indicating that the nanoparticles show a preferred separation distance.

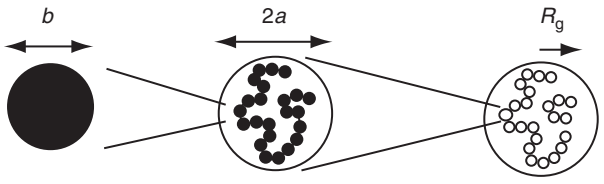

Figure 5 Fractal aggregate composed of primary particles of size b showing self-similarity in the fractal-scaling regime, $b < 2a < 2R_g$. Adapted from Beaucage, G. *J. Appl. Cryst.* **1996**, *29*, 134–146, Figure 4.[22] (Circles in the right cartoon are composed of the aggregates in the middle cartoon.)

of free parameters. For example, a two-level structure would display eight free parameters, G_i, $R_{g,i}$, B_i, and P_i for each level. If a sample is known to be composed of polydisperse rods with aspect ratios larger than about 2.5, then we know that the smallest structural level, level 1, will display $P = 4$ for a smooth, sharp surface and the larger level, level 2, will display $P = 1$ for linear scaling between the diameter and the length of the rod. This leaves six free parameters. The smallest level radius of gyration for the rod of radius, R, is $R_{g,1}^2 = 3R^2/4$ and for the larger level is $R_{g,2}^2 = L^2/12 + R^2/2$. The scaling prefactor for level 2 is $B_2 = \pi G_2/L$ and for level 1 is $B_1 = G_1/(R^3 L)$.[1,2] Generally, $G_{i+1} = zG_i$, where z is the weight average number of subunits of type 'i' in the structure '$i+1$'.[22] For a rod, $G_2 = (3L/R)G_1$. Scattering for the rod hierarchical structure is determined by three parameters: R, L, and a contrast factor G_1. Similarly, three parameters determine the two-level hierarchical scattering from disks. **Table 1** lists the free parameters and values for each of the four parameters in each structural level for a variety of

Table 1 Values of the Unified Equation Parameters for a number of structural models

Structural model	*Free parameters*	*G*	R_g^2	*B*	*P*	*References*
Sphere	R, G_1	G_1	$\frac{3}{5}R^2$	$\frac{9G_1}{(2R^4)}$	4	24, 25
Polydisperse particles	$R_{g,1}$, G_1, $\mathrm{PDI} = \frac{R_g^4 B_1}{1.62 G_1}$	G_1	$\frac{3\langle R_1^8\rangle}{5\langle R_1^6\rangle} = \left(\frac{1.62 G_1 \mathrm{PDI}_1}{B_1}\right)^{\frac{1}{2}}$	$\frac{9G_1\langle R_1^2\rangle}{2\langle R_1^6\rangle} = \frac{1.62 G_1 \mathrm{PDI}_1}{R_{g,1}^4}$	4	24, 25
Rod($L > 2.5\ R$)	R, L, G_1	G_1	$\frac{3R^2}{4}$	$\frac{2G_1}{R^2 L^2}$	4	1, 2
		$G_2 = G_1 \frac{3\pi L}{4R}$	$\frac{L^2}{12} + \frac{R^2}{2}$	$\frac{\pi G_2}{L}$	1	
Disk ($D > 2.5\,t$)	R, t, G_1	G_1	$\frac{t^2}{4}$	$\frac{2G_1}{R^2 t^2}$	4	1, 2
		$G_2 = G_1 \frac{3\pi t}{4R}$	$\frac{t^2}{12} + \frac{R^2}{2}$	$\frac{2G_2}{R^2}$	2	
Monodisperse, linear polymer	l_p, z, G_1, k	G_1	$\frac{l_p^2}{3}$	$\frac{\pi G_1}{2 l_p}$	1	6, 26–28
		$G_2 = zG_1$	$\frac{4kz^{2/d_f} l_p^2}{\left(1+\frac{2}{d_f}\right)\left(2+\frac{2}{d_f}\right)}$	$\frac{z d_f G_1 \Gamma\left(\frac{d_f}{2}\right)}{R_{g,2}^{d_f}}$	d_f	
Gel-tensile blob model	l_p, G_1, L, χ $\xi = \frac{l_p}{(1-2\chi)^D}$ $D \cong \frac{1}{17}$	G_1	$\frac{l_p^2}{3}$	$\frac{\pi G_1}{2 l_p}$	1	3, 4
		$G_2 = kG_1\left(\frac{\xi}{2l_p}\right)^{5/3}$	$\frac{25\xi^2}{176}$	$\frac{3G_2\Gamma\left(\frac{5}{6}\right)}{R_{g,2}^{5/3}}$	5/3	
		$G_3 = G_2\left(\frac{L}{\xi}\right)$	$\frac{L^2}{12} + \frac{\xi^2}{8}$	$\frac{G_1\Gamma\left(\frac{1}{2}\right)}{R_{g,3}}$	1	
Polydisperse branched polymer in good solvent	$d_f = cd_{\min}$ $d_{\min}$, c, G_1, z, k, C_p.	G_1	$\frac{l_p^2}{3}$	$\frac{\pi G_1}{2 l_p}$	1	6, 26–29
		$G_2 = zG_1$	$\frac{4kz^{2/d_f} l_p^2}{\left(c+\frac{2}{d_{\min}}\right)\left(1+c+\frac{2}{d_{\min}}\right)}$	$\frac{z d_{\min} G_1 C_p \Gamma\left(\frac{d_f}{2}\right)}{R_{g,2}^{d_f}}$	d_f	
Cyclic polymer	$d_{\min} = d_f(1 - \ln 2/\ln z)$ z, G_1, l_p, k, $d_f = 2.12$	G_1	$\frac{l_p^2}{3}$	$\frac{\pi G_1}{2 l_p}$	1	11
		$G_2 = zG_1$	$\frac{4k(z/2)^{2/d_f} l_p^2}{\left(c+\frac{2}{d_{\min}}\right)\left(1+c+\frac{2}{d_{\min}}\right)}$	$\frac{z d_{\min} G_1 C_p \Gamma\left(\frac{d_f}{2}\right)}{R_{g,2}^{d_f}}$	2.12	
Polydisperse branched fractal aggregates with agglomerates	G_1, z, N_{Agg}, k, C_p	G_1	$\frac{3\langle R_1^8\rangle}{5\langle R_1^6\rangle} = \left(\frac{1.62 G_1 \mathrm{PDI}_1}{B_1}\right)^{\frac{1}{2}}$	$\frac{9G_1\langle R_1^2\rangle}{2\langle R_1^6\rangle} = \frac{1.62 G_1 \mathrm{PDI}_1}{R_{g,1}^4}$	4	19, 24, 25, 29
		$G_2 = zG_1$	$\frac{kz^{2/d_f} d_p^2}{\left(c+\frac{2}{d_{\min}}\right)\left(1+c+\frac{2}{d_{\min}}\right)}$	$\frac{z d_{\min} G_1 C_p \Gamma\left(\frac{d_f}{2}\right)}{R_{g,2}^{d_f}}$	d_f	
		$G_3 = N_{Agg}\ G_2$	$\frac{3\langle R_3^8\rangle}{5\langle R_3^6\rangle} = \left(\frac{1.62 G_3 \mathrm{PDI}_3}{B_3}\right)^{\frac{1}{2}}$	$\frac{9G_3\langle R_3^2\rangle}{2\langle R_3^6\rangle} = \frac{1.62 G_3 \mathrm{PDI}_3}{R_{g,3}^4}$	4	

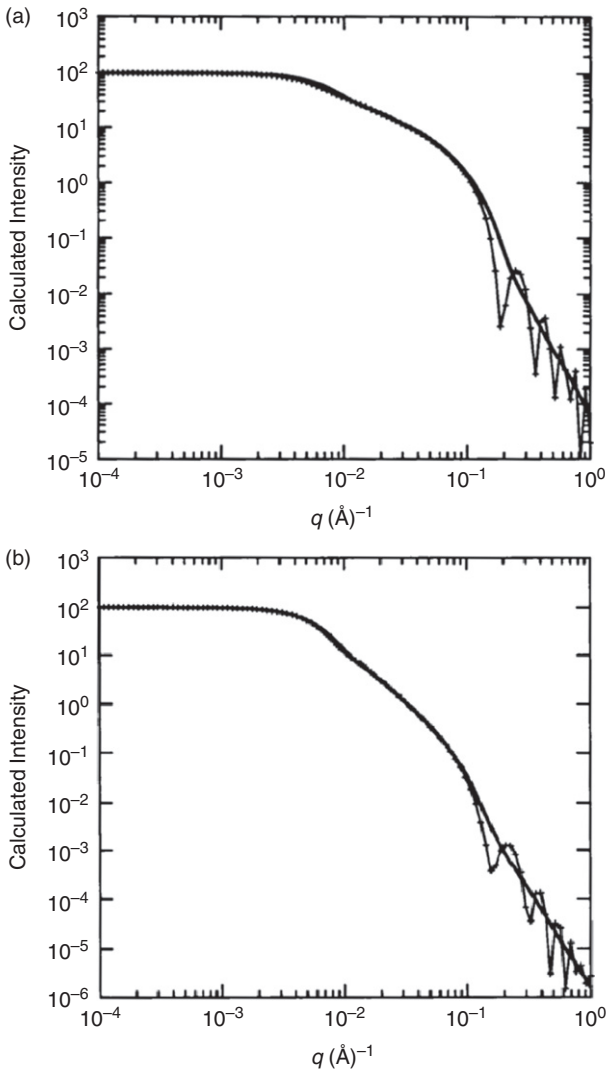

Figure 6 (a) Unified calculation compared to calculation for polydisperse rods with two structural levels, rod diameter and rod length. (b) Unified calculation compared to calculation for polydisperse disks with two structural levels, disk thickness and disk diameter. Adapted from Beaucage, G. *J. Appl. Cryst.* **1995**, *28*, 717–728, Figures 13 and 14.[1] In both cases, the dark line is the unified calculation.

structural models. Figure 6 shows eqn [11] compared with exact scattering functions for rods and disks using the parameters listed in Table 1. The exact functions display oscillations associated with the monodisperse structural sizes. Equation [11] does not display these oscillations but follows the gross scaling and size features for these structures.

Equation [11] can be modified in cases where the cut-off radius of gyration differs from the substructural radius of gyration such as shown in Figure 7. In this case eqn [11] becomes,[1,2]

$$I(q) = \left(G_2 \exp\left(\frac{-q^2 R_{g,2}^2}{3}\right) + B_2 \exp\left(\frac{-q^2 R_{sub}^2}{3}\right) q_2^{*P_2}\right) + \left(G_1 \exp\left(\frac{-q^2 R_{g,1}^2}{3}\right) + B_1 q_1^{*P_1}\right) \quad [13]$$

This approach has proven useful in some studies of carbon black in polymer matrices.[30]

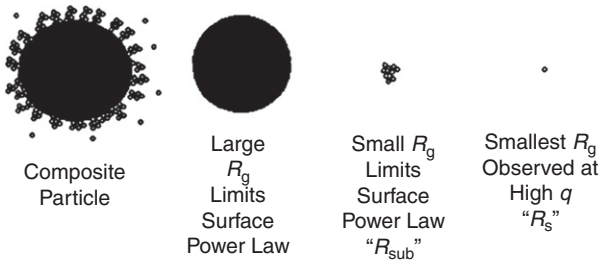

Figure 7 Schematic of particles composed of subparticles with a radius of gyration for the entire particle, $R_{g,2}$, and a radius of gyration for the subparticles, $R_{g,1}$, are observed, but the cut-off radius, R_{sub}, differs from $R_{g,1}$. Generally, $R_{g,1} = R_{sub}$. Adapted from Beaucage, G. *J. Appl. Cryst.* **1995**, *28*, 717–728, Figure 9.[1]

2.14.6 Examples of Structural Models and the Unified Function

Several examples of the application of eqn [11] to experimental data are shown below. Figure 8(**a**) shows a fit to scattering from branched polyethylene in dilute solution that displays close to good-solvent scaling.[6,26] The model fits two structural levels, the Kuhn length, which is monotonic in short-chain branching, and the chain coil that shows changes with long-chain branching. From this global fit, it is possible to calculate the number of short-chain branches, number of long-chain branches, chain polydispersity (M_z/M_w), the hyperbranch (branch on branch) content, the mole fraction branches, and the average branch length[6,26,27] using the unified function and a branching model. A similar approach can be used for fractal aggregates.[19]

Figure 9(**a**) shows a combination of light scattering and X-ray scattering data for glass microfiber nonwovens.[28] Light scattering was performed in benzyl alcohol that almost contrast matches silica. The data are fitted to two structural levels. The microfibers display Porod scattering at high q and a self-avoiding walk at larger sizes, $d_f = 5/3$, analogous to polymers in good solvent (Figure 8(**a**)). Figure 9(**b**) shows X-ray scattering from surface-fractal aggregates of carbon black in polymethyl methacrylate. The primary particles display turbostratic graphitic structure at high q reflected by a power-law −2 regime. The scattering near $q = 1$ Å^{-1} is diffraction from the graphitic carbon nanoparticles.

Figure 10 shows SAXS from two hierarchical structures in polyacrylonitrile and isotactic polystyrene foams produced by supercritical extraction of semicrystalline polymer gels.[31,32] Both foams display three structural levels, the first two of which correspond to uncorrelated lamellar crystals and follow the parameters listed in Table 1 for lamellar scattering. The lamellae compose larger-scale structures that are apparent in the micrographs of Figures 10(**c**) and 10(**d**). For the ball morphology, the low-q structural level follows sphere scattering.

2.14.7 Polydispersity and Asymmetry for Porod Scattering

For structures that display Porod scattering, following eqn [2] with $P = 4$, a relationship exists between the Porod prefactor, B,

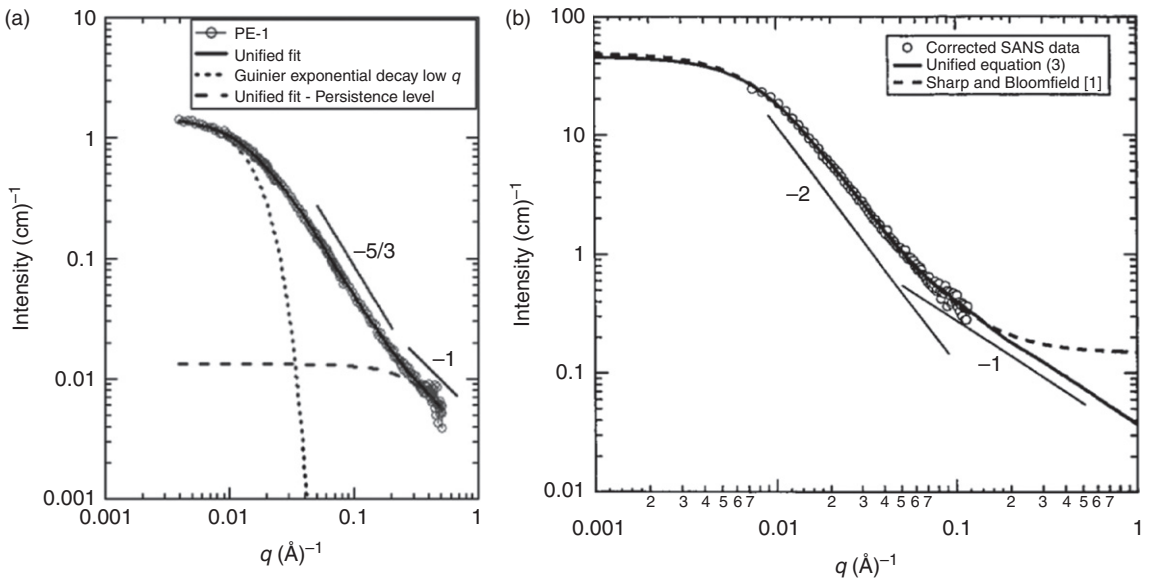

Figure 8 Unified fit to two SANS data. (a) From polyethylene samples in D-paraxylene showing good-solvent and Kuhn scaling. Adapted from Ramachandran, R.; Beaucage, G.; Kulkarni, A. S.; *et al. Macromolecules* **2008**, *41*, 9802–9806, Figure 1,[6] showing close to good-solvent scaling. (b) From D-polyhydroxybutyrate (PHB) in hydrogenous PHB (adapted from Beaucage, G.; Rane, S.; Sukumaran, S.; *et al. Macromolecules* **1997**, *30*, 4158–4162, Figure 3[5]) showing Gaussian scaling. The solid line is the unified fit composed of two structural levels, coil scaling at low q and persistence at high q, –1 power-law slope.

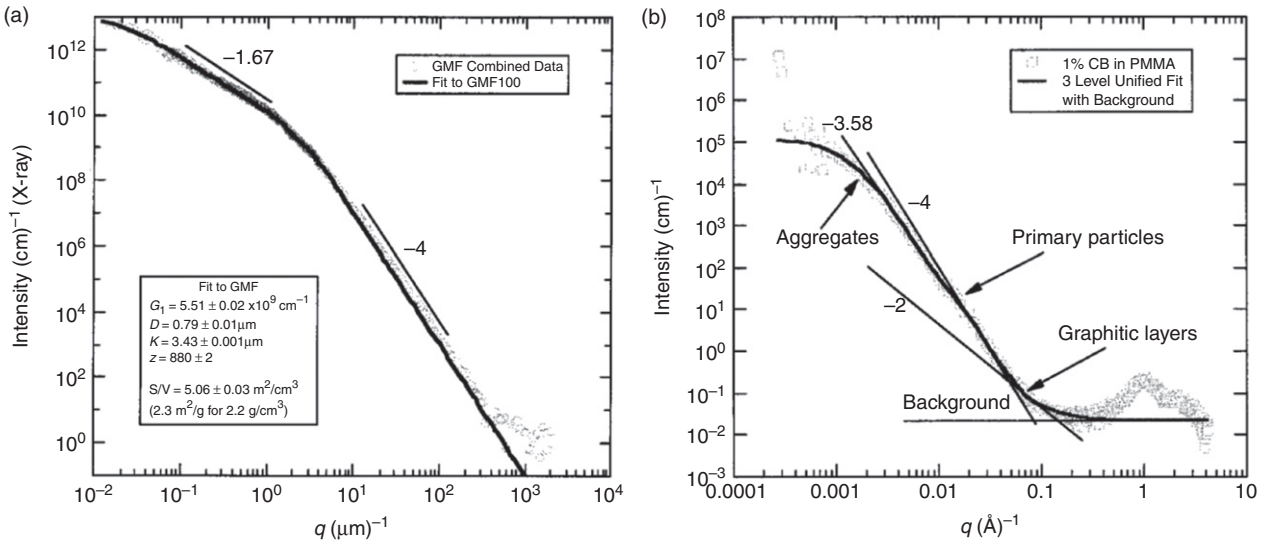

Figure 9 (a) Light and X-ray scattering from a nonwoven glass microfiber mat. Adapted from Beaucage, G.; Sukumaran, S.; Rane, S.; Kohls, D.J. *J. Polym. Sci.: Polym. Phys.* **1998**, *36*, 3147–3154, Figure 2.[28] Two structural levels are displayed, a self-avoiding walk at low q and Porod surface scattering at high q. (b) Scattering from carbon black in a polymethyl methacrylate (PMMA) matrix showing three structural levels. Adapted from Beaucage, G.; Rane, S.; Schaefer, D. W.; et al. *J. Polym. Sci.: Polym. Phys.* **1999**, *37*, 1105–1119, Figure 8.[34] At low q, rough-surfaced solid aggregates are observed, power-law decay of –3.58; at intermediate q, Porod surface scattering is observed from the primary particles; and at high q, a –2 decay reflecting 2D graphitic layers is observed.

and the polydispersity and asymmetry of the structures. Monodisperse spherical particles display a minimum in B relative to G,[24,25]

$$B_{\text{monodisperse,sphere}} = \frac{81G}{50R_g^4} = \frac{1.62G}{R_g^4} \qquad [14]$$

The ratio $\text{PDI} = BR_g^4/1.62G$ is a scattering polydispersity index (PDI) that ranges from 1 for monodisperse spheres to a maximum of about 9. For particles displaying a log-normal distribution in size, there is a simple relationship between PDI and the standard deviation and geometric standard deviation,

$$\sigma = \ln \sigma_g = \left(\frac{\ln \text{PDI}}{12}\right)^{1/2} \quad \text{and} \quad m = \left\{\frac{5R_g^2}{3\exp(14\sigma^2)}\right\}^{1/2} \qquad [15]$$

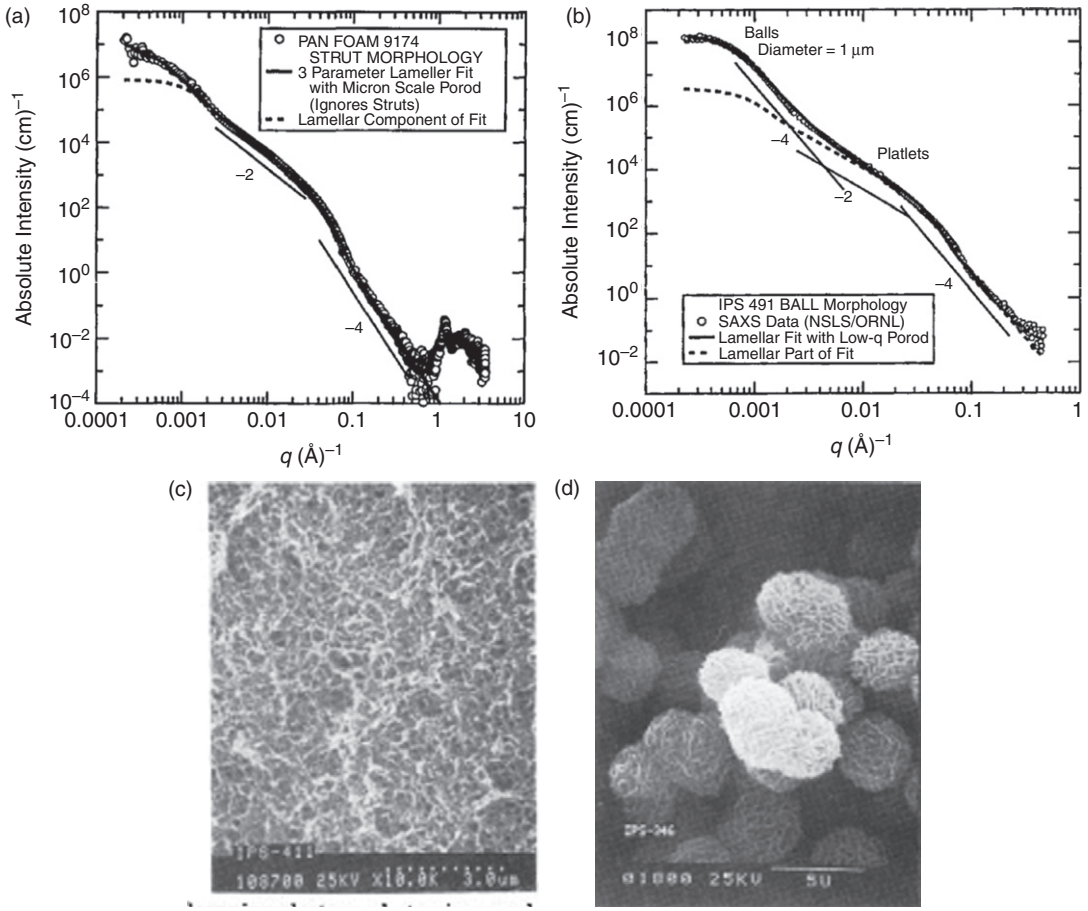

Figure 10 Polyacrylonitrile and isotactic polystyrene structures composed of uncorrelated lamellar crystals produced by supercritical extraction of semicrystalline gels. (a) and (c) correspond to 'strut' morphology, while (b) and (d) correspond to 'ball' morphology. Data are fit using the unified function with three structural levels in increasing size scale: a lamellar model for levels 1 and 2 and a Porod regime for level 3. For the 'ball' morphology, spherical restrictions were used for level 3. (a and b) Adapted from Beaucage, G.; Aubert, J. H.; Lagasse, R. R.; et al. *J. Polym. Sci.: Polym. Phys.* **1996**, *34*, 3063–3072.[31] Figures 2 and 8, and (c and d) adapted from Aubert, J. H. *Macromolecules* **1988**, *21*, 3468–3473, Figure 9.[32]

where m is the median particle radius and the mean radius is given by $\langle R\rangle = m\exp(\sigma^2/2)$.[24] The Sauter mean diameter, d_p, can be obtained from the invariant, $Q = \int_0^\infty q^2 I(q)\mathrm{d}q$ and B,

$$d_p = \frac{6Q}{\pi B} = \frac{6\ \langle V\rangle}{\langle S\rangle} \qquad [16]$$

Figure 11 compares the log-normal distribution for titania nanoparticles obtained from the unified function with a direct particle counting using transmission electron microscopy (TEM) and with a SAXS data conversion using the maximum entropy method.

2.14.8 Restrictions for the Unified Function Parameters

The parameters in eqn [11] are limited to a viable range of values due to certain physical limits. P is limited to $1 \le P \le$ approximately 5. For scattering that follows Porod's law, $P = 4$, the power-law prefactor must follow,

$$\frac{1.62G}{BR_g^4} \le B_{\mathrm{Porod}} \le \text{approximately } 9 \qquad [17]$$

For a linear polymer,[22]

$$\frac{BR_g^{d_f}}{\Gamma\left(\frac{d_f}{2}\right)} = d_f \quad \text{and} \quad 1 = \frac{d_f\Gamma\left(\frac{d_f}{2}\right)}{BR_g^{d_f}} \qquad [18]$$

For a regular object (disk, rod, sphere),

$$\frac{BR_g^{d_f}}{\Gamma\left(\frac{d_f}{2}\right)} = 1 \qquad [19]$$

For any fractal structure,[29] $1 \le d_f < 3$,

$$1 \le \frac{BR_g^{d_f}}{\Gamma\left(\frac{d_f}{2}\right)} \le d_f \quad \text{and} \quad 1 \le \frac{d_f\Gamma\left(\frac{d_f}{2}\right)}{BR_g^{d_f}} \le d_f \qquad [20]$$

When the second expression in eqn [20] is not followed, the fractal structures may be highly polydisperse in size. It is possible to account for this polydispersity as described in References 19, 26, and 27.

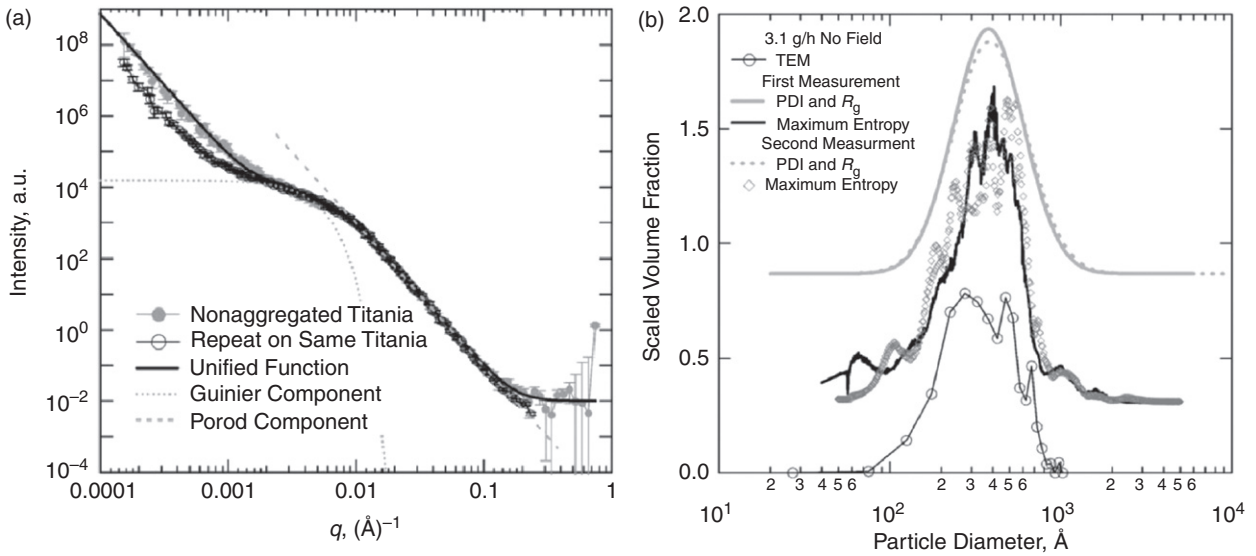

Figure 11 (a) SAXS from titania nanoparticles and unified fit. $d_p = 34.9$ nm, PDI = 14.4, $R_g = 44.2$ nm. (b) Particle size distribution for titania unified analysis of Porod regime, TEM particle counting, and a scattering integral method. Adapted from Beaucage, G.; Kammler, H. K.; Pratsinis, S. E. *J. Appl. Cryst.* **2004**, *37*, 523–535, Figures 5(a) and 5(b).[24]

2.14.9 Software for Unified Fits

A useful software for unified fits has been written by Jan Ilavsky at the Advanced Photon Source, Argonne National Laboratories. This software is available for download at http://usaxs.xor.aps.anl.gov/staff/ilavsky/irena.html. The code requires the Igor Pro program. A trial version of Igor Pro can be obtained at www.wavemetrics.com.

2.14.10 Conclusion

This section has briefly outlined the uses of the unified function for modeling hierarchical structures in small-angle scattering. A short overview of models that describe a single structural level was given and the unified function was described. Coupling of a wide range of structural models to the unified parameters was presented. This is not an exhaustive list. Use of the unified function to determine particle size distributions was demonstrated and some general restrictions to the fitting parameters were presented.

The unified function has proven useful to understand small-angle scattering from disordered systems displaying complex structures. It has even shown use in understanding the transition from disordered, unfolded state in proteins and RNA to the folded state.[33] However, the function is not applicable to systems that display high degrees of regularity such as native-state proteins or monodisperse particulates. There is also some danger in the application of the unified function without taking heed of the limitations to the fitting parameters mentioned above, particularly restrictions in the Porod regime on the power-law prefactor. While we have demonstrated that the function can be used in quite highly polydisperse systems both for fractal[26,27] and solid particulate systems,[19,24,25] some care must be taken in the analysis of these systems. Further, it is generally not possible to distinguish between asymmetry and polydispersity in scattering data and care should be take in the analysis of data that displays both asymmetric particles and high degrees of polydispersity.[34]

References

1. Beaucage, G. *J. Appl. Cryst.* **1995**, *28*, 717–728.
2. Beaucage, G.; Schaefer, D. W. *J. Non-Cryst. Solids* **1994**, *172–174*, 797–805.
3. Sukumaran, S. K.; Beaucage, G. *Europhys. Lett.* **2002**, *59*, 714–720.
4. Sukumaran, S. K.; Beaucage, G.; Mark, J. E.; Viers, B. *Eur. Phys. J. E* **2005**, *18*, 29–36.
5. Beaucage, G.; Rane, S.; Sukumaran, S.; *et al. Macromolecules* **1997**, *30*, 4158–4162.
6. Ramachandran, R.; Beaucage, G.; Kulkarni, A. S.; *et al. Macromolecules* **2008**, *41*, 9802–9806.
7. Flory, P. J. *Statistical Mechanics of Chain Molecules*; Cornell University Press: Ithaca, NY, 1969.
8. Benoit, H. *J. Polym. Sci.* **1953**, *11*, 507.
9. Benoit, H. *Compt. Rend.* **1957**, *245*, 2244–2247.
10. Casassa, E. *J. Polym. Sci., Part A* **1965**, *3*, 605–614.
11. Beaucage, G.; Kulkarni, A. S. *Macromolecules* **2010**, *43*, 532–537.
12. Debye, P.; Bueche, A. M. *J. Appl. Phys.* **1949**, *20*, 518–525.
13. Sorensen, C. M.; Wang, G. M. *Phys. Rev. E* **1999**, *60*, 7143–7148.
14. Sinha, S. K.; Freltoft, T.; Kjems, J. In *Kinetics of Aggregation and Gelation*; Family, F., Landau, D. P., Eds.; North-Holland: Amsterdam, Netherlands, 1984; pp 87–90.
15. Teixeira, J. *J. Appl. Cryst.* **1988**, *21*, 781–785.
16. Debye, P.; Anderson, H. R.; Brumberger, H. *J. Appl. Phys.* **1957**, *28*, 679–683.
17. Sinha, S. K. *Physica D* **1989**, *38*, 310–314.
18. Teixeira, J. In *On Growth and Form: Fractal and Non-Fractal Patterns in Physics*; Stanley, H. E., Ostrowsky, N., Eds.; Martinus Nijhoff Publishers: Dordrecht, Netherlands, 1985; pp 145–162.
19. Rai, D. K.; Ramachandran, R.; Beaucage, G. In preparation.
20. Svergun, D. I.; Koch, M. H. J. *Rep. Prog. Phys.* **2003**, *66*, 1735–1782.
21. Koch, M. H. J.; Vachette, P.; Svergun, D. I. *Quat. Rev. Biophys.* **2003**, *36*, 147–227.
22. Beaucage, G. *J. Appl. Cryst.* **1996**, *29*, 134–146.
23. Beaucage, G.; Ulibarri, T. A.; Black, E. P.; Schaefer, D. W. In *Hybrid Organic-Inorganic Composites ACS Symposium Series 585*; Mark, J. E., Lee, C. Y.-C., Bianconi P. A., Eds.; American Chemical Society: Washington, DC, 1995; pp 97–111.
24. Beaucage, G.; Kammler, H. K.; Pratsinis, S. E. *J. Appl. Cryst.* **2004**, *37*, 523–535.
25. Kammler, H. K.; Beaucage, G.; Kohls, D. J.; *et al. J. Appl. Phys.* **2005**, *97*, 54309.
26. Ramachandran, R.; Beaucage, G.; Kulkarni, A. S.; *et al. Macromolecules* **2009**, *42*, 4746–4750.

27. Ramachandran, R.; Beaucage, G.; McFaddin, D.; *et al. Polymer* **2011**, *52*, 2661–2666.
28. Beaucage, G.; Sukumaran, S.; Rane, S.; Kohls, D. J. *J. Polym. Sci.: Polym. Phys.* **1998**, *36*, 3147–3154.
29. Beaucage, G. *Phys. Rev. E* **2004**, *70*, 31401.
30. Koga, T.; Hashimoto, T.; Takenaka, M.; *et al. Macromolecules* **2008**, *41*, 453–464.
31. Beaucage, G.; Aubert, J. H.; Lagasse, R. R.; *et al. J. Polym. Sci.: Polym. Phys.* **1996**, *34*, 3063–3072.
32. Aubert, J. H. *Macromolecules* **1988**, *21*, 3468–3473.
33. Beaucage, G. *Biophys. J.* **2008**, *95*, 503–508.
34. Beaucage, G.; Rane, S.; Schaefer, D. W.; *et al. J. Polym. Sci.: Polym. Phys.* **1999**, *37*, 1105–1119.

Biographical Sketch

Dr. Greg Beaucage has worked in the field of SAXS, small-angle neutron scattering (SANS), and light scattering for more than two decades, first during graduate school in the Polymer Science Program at the University of Massachusetts, Amherst, and later at Sandia National Laboratory, and finally at the University of Cincinnati where he is currently a professor in the Department of Chemical and Materials Engineering. Beaucage has more than 110 peer-reviewed publications with an *H*-index of 29. Many of Beaucage's publications deal with scattering theory including several papers developing the unified function that is used in understanding scattering from hierarchical structures. Beaucage is a fellow of the American Physical Society and is a former chair of the small-angle scattering special interest group for the American Crystallographic Association. Beaucage was a founding member of the Center for Advanced Microstructures and Devices synchrotron at Louisiana State University and has served on the advisory board of the Intense Pulsed Neutron Source at Argonne National Laboratory and is a member of the user advisory board for Spallation Neutron Source and High Flux Isotope Reactor at Oak Ridge National Laboratory. Beaucage was a visiting faculty at the Eidgenössiche Technische Hochschule Zürich (ETHZ) in Zürich, Switzerland, during 2003 and was a visiting faculty in the Department of Physics at the University of Cape Town during 2011. Currently, Beaucage is interested in the quantification of molecular topology using SANS in work funded by LyondellBasell and Exxon, in the hierarchical structure of ceramic and metallic aggregates in work funded by the US National Science Foundation and the US Department of State through the Agency for International Development's Higher Education for Development program and in the study of protein structure using SAXS. Beaucage is a frequent user of the Advanced Photon Source in Chicago and other synchrotron facilities as well as neutron scattering facilities at Oak Ridge and National Institute of Standards and Technology. Beaucage's laboratory at the University of Cincinnati is equipped with five SAXS instruments including pinhole, Kratky, and Bonse–Hart cameras.